Available online at www.sciencedirect.com

SciVerse ScienceDirect

Journal of Nutritional Biochemistry 23 (2012) 591–601

Journal of Nutritional Biochemistry

The curry spice curcumin selectively inhibits cancer cells growth *in vitro* and in preclinical model of glioblastoma☆

Alfeu Zanotto-Filho[a,*], Elizandra Braganhol[b], Maria Isabel Edelweiss[c], Guilherme A. Behr[a], Rafael Zanin[b], Rafael Schröder[a], André Simões-Pires[a], Ana Maria Oliveira Battastini[b], José Cláudio Fonseca Moreira[a]

[a]*Centro de Estudos em Estresse Oxidativo, Departamento de Bioquímica, Universidade Federal do Rio Grande do Sul (UFRGS), Porto Alegre, Rio Grande do Sul, Brasil*
[b]*Laboratório de Enzimologia, Departamento de Bioquímica, Universidade Federal do Rio Grande do Sul (UFRGS), Porto Alegre, Rio Grande do Sul, Brasil*
[c]*Laboratório de Patologia, Hospital de Clínicas de Porto Alegre (HCPA), Porto Alegre, Rio Grande do Sul, Brasil*

Received 14 December 2010; received in revised form 30 January 2011; accepted 24 February 2011

Abstract

Previous studies suggested that curcumin is a potential agent against glioblastomas (GBMs). However, the *in vivo* efficacy of curcumin in gliomas remains not established. In this work, we examined the mechanisms underlying apoptosis, selectivity, efficacy and safety of curcumin from *in vitro* (U138MG, U87, U373 and C6 cell lines) and *in vivo* (C6 implants) models of GBM. *In vitro*, curcumin markedly inhibited proliferation and migration and induced cell death in liquid and soft agar models of GBM growth. Curcumin effects occurred irrespective of the p53 and PTEN mutational status of the cells. Interestingly, curcumin did not affect viability of primary astrocytes, suggesting that curcumin selectivity targeted transformed cells. In U138MG and C6 cells, curcumin decreased the constitutive activation of PI3K/Akt and NFkappaB survival pathways, down-regulated the antiapoptotic NFkappaB-regulated protein bcl-xl and induced mitochondrial dysfunction as a prelude to apoptosis. Cells developed an early G2/M cell cycle arrest followed by sub-G1 apoptosis and apoptotic bodies formation. Caspase-3 activation occurred in the p53-normal cell type C6, but not in the p53-mutant U138MG. Besides its apoptotic effect, curcumin also synergized with the chemotherapeutics cisplatin and doxorubicin to enhance GBM cells death. In C6-implanted rats, intraperitoneal curcumin (50 mg kg^{-1} d^{-1}) decreased brain tumors in 9/11 (81.8%) animals against 0/11 (0%) in the vehicle-treated group. Importantly, no evidence of tissue (transaminases, creatinine and alkaline phosphatase), metabolic (cholesterol and glucose), oxidative or hematological toxicity was observed. In summary, data presented here suggest curcumin as a potential agent for therapy of GBMs.
© 2012 Elsevier Inc. All rights reserved.

Keywords: Curcumin; Glioblastoma; Apoptosis; *In vitro*; Preclinical

1. Introduction

Glioblastoma (GBM) is an aggressive, invasive and difficult to treat primary brain tumor. Standard therapy includes surgical resection, external beam radiation and chemotherapy, with no known curative therapy [1,2]. A number of deregulated signaling cascades have been described in GBMs, including the nuclear factor kappa-B (NFkappaB), the phosphoinositide-3-kinase (PI3K/Akt) pathway and the Ras/MEK/ERK mitogen-activated protein kinase pathway. Deregulation of these pathways is driven by mutation, amplification or overexpression of multiple genes such as PTEN, EGFr, PDGFR-a, p53 and mTOR [3–5]. Understanding these deregulated pathways has provided the basis for designing molecular targeted therapies as well as new combination therapies and drug delivery systems [6–8]. Despite the aforementioned findings, median survival in GBM has remained approximately 1 year for decades [1,2]. Therefore, validation of new antiglioma drugs may offer new therapeutic opportunities to patients.

Curcumin (diferuloylmethane), a naturally occurring polyphenol derived from the root of the rhizome *Curcuma longa*, possesses anti-inflammatory, antioxidant and anticancer properties by inhibition of signaling pathways such as NFkappaB, PI3K/Akt and activator protein-1 (AP-1) [9]. Recently, curcumin entered into phase I clinical trials for the treatment of some high-risk cancers [10]. In GBMs, an emerging *in-vitro*-based literature [11–16] suggests that curcumin exerts antiglioma effects through enhancement of TRAIL-induced apoptosis [11], inhibition of metalloproteinase-9 expression [12,14] and induction of apoptosis in T98G and U87MG cell lines [13,15,16]. However, the apoptotic mechanisms, selectivity to transformed cells and principally the *in vivo* efficacy of curcumin in GBMs remain to be better studied. In this work, we examined the mechanisms underlying curcumin anti-GBM effects based on *in vitro* (C6, U138MG, U87 and U373 cell lines) and *in vivo* (C6 implants in rat brain) models of the disease. *In vitro*, we evaluated curcumin effects on proliferation, apoptosis and migration as well as antagonism with classical GBM survival pathways (PI3K/Akt and NFkappaB), selectivity to cancer

☆ Conflict of interest statement: The authors report that there are no conflicts of interest.

* Corresponding author. Depto. Bioquímica (ICBS-UFRGS), Rua Ramiro Barcelos, 2600/Anexo, CEP 90035-003, Porto Alegre, Rio Grande do Sul, Brazil. Tel.: +55 51 3308 5578; fax: +55 51 3308 5535.

E-mail address: alfeuzanotto@hotmail.com (A. Zanotto-Filho).

0955-2863/$ - see front matter © 2012 Elsevier Inc. All rights reserved.
doi:10.1016/j.jnutbio.2011.02.015

cells and adjuvant potential. *In vivo*, we tested the hypothesis that curcumin may decrease glioma growth without inducing toxicity to healthy tissues.

2. Materials and methods

2.1. Reagents

Curcumin, propidium iodide (PI), Hepes, CHAPS, dithiothreitol, EDTA, trypsin, 3-(4,5-dimethyl)-2,5-diphenyl tetrazolium bromide (MTT), Nonidet-P40, spermin tetrahydrochloride, RNAse A and culture analytical-grade reagents were purchased from Sigma Chemical Co. (St. Louis, MO, USA). Anti-lamin B (C-20) and anti-p65 NFkappaB antibodies were from Santa Cruz Biotechnologies; anti-β-actin, anti-phospho-Akt(ser^{473}) , anti-Akt and anti-bcl-xl were from Cell Signaling Technology. Parthenolide (PTL) and LY294002 were from Biomol International (Plymouth Meeting, PA, USA). Electrophoresis and immunoblotting reagents were from Bio-Rad Laboratories (Hercules, CA, USA). Kits for biochemical analysis were acquired from Labtest Diagnostica (MG, Brazil).

2.2. Cell cultures

The rat (C6) and human (U138MG, U87 and U373) malignant GBM cell lines were obtained from American Type Culture Collection (Rockville, MD, USA). The cells were grown and maintained in low-glucose Dulbecco's modified Eagle's medium (DMEM; Gibco BRL, Carlsbad, CA, USA) containing 0.1% Fungizone and 100 U/L gentamicin and supplemented with 10% fetal bovine serum (FBS). Cells were kept at 37°C in a humidified atmosphere with 5% CO_2. Primary astrocyte cultures were prepared as previously described [17]. Briefly, cortex of newborn Wistar rats (1–2 days old) were removed and dissociated mechanically in a Ca^{+2} and Mg^{+2} free balanced salt solution, pH 7.4, (137 mmol/L NaCl, 5.36 mmol/L KCl, 0.27 mmol/L Na_2HPO4, 1.1 mmol/L KH_2PO4, 6.1 mmol/L glucose). After centrifugation at 1000 rpm for 5 min, the pellet was resuspended in DMEM supplemented with 10% FBS. The cells (2×10^5) were plated in poly-L-lysine-coated 48-well plates. After 4-h plating, plates were gently shaken and phosphate-buffered saline (PBS)-washed, and medium was changed to remove neuron and microglia contaminants. Cultures were allowed to grow to confluence by 20–25 days. Medium was replaced every 4 days.

2.3. MTT and lactate dehydrogenase assays

Dehydrogenases-dependent MTT reduction (MTT assay) and lactate dehydrogenase release into culture medium [lactate dehydrogenase (LDH) assay] were used as an estimative of cell viability [18]. Cells were plated in 96-well plates (10^4/well) and treated at 60%–70% confluence. At the end of incubations, MTT and LDH assays were performed. Lactate dehydrogenase activity in the culture medium was determined in agreement with manufacturer instructions (CytoTox 96-NonRadioactive Cytotoxicity Assay, Promega). Cell morphology was evaluated by light microscopy (Nikon Eclipse TE 300).

2.4. PI incorporation and staining of chromatin

For determination of PI uptake in cells with losses in membrane integrity, treated cells were incubated with 2 μg/ml PI in complete medium for 1 h. Propidium iodide fluorescence was excited at 515–560 nm using an inverted microscope (Nikon Eclipse TE 300) fitted with a standard rhodamine filter. Representative microphotographs (at least five per well) were collected [19]. For detection of the morphological alterations in chromatin (condensation and fragmentation) and apoptotic bodies formation, cells were fixed in methanol/acetone (1:1) for 5 min and washed with PBS (three times). Afterward, chromatin was stained with PI (0.5 μg/ml, 10 min) followed by fluorescent microscopy (Nikon Eclipse TE 300).

2.5. Cell cycle analysis

For cell cycle analysis, cells were trypsinized, centrifuged and resuspended in a lysis buffer containing 3.5 mmol/L trisodium citrate, 0.1% vol/vol Nonidet P-40, 0.5 mmol/L Tris-HCl, 1.2 mg/ml spermine tetrahydrochloride, 5 μg/ml RNAse, 5 mmol/L EDTA and 1 μg/ml PI, pH 7.6. Afterward, cells were incubated for at least 10 min on ice for cell lysis. DNA content was determined by flow cytometry. Ten thousand events were counted per sample. FACS analyses were performed in the CellQuest Pro Software (BD Biosciences, CA, USA) [18].

2.6. Caspase-3 activity

Caspase-3 activity was assessed in agreement with CASP3F Fluorometric kit (Sigma, Saint Louis, MI, USA). Treated cells were harvested and incubated in a lysis buffer (50 mmol/L Hepes, 5 mmol/L CHAPS and 5 mmol/L dithiothreitol, pH 7.4) for 20 min in ice. Afterward, extracts were clarified by centrifugation at 13,000*g* (15 min, 4°C). Supernatants were collected, and proteins were measured by Bradford method. For assays, 150 μg proteins were mixed with 200 μl of the assay buffer (20 mmol/L Hepes, 0.1% CHAPS, 5 mmol/L dithiothreitol, 2 mmol/L EDTA, pH 7.4) plus 20 μM Ac-DEVD-AMC (Acetyl-Asp-Glu-Val-Asp-7-amido-4-methylcoumarin), a caspase-3-specific substrate. Caspase-3-mediated substrate cleavage was monitored during 1 h (37°C) in a fluorometric reader (excitation 360 nm/emission 460 nm) [18].

2.7. Cellular fractionation

For nuclear extracts preparation, cells (~5×10^6, 70%–80% confluence) were washed with cold PBS and suspended in 0.4-ml hypotonic lysis buffer [10 mmol/L HEPES (pH 7.9), 1.5 mmol/L $MgCl_2$, 10 mmol/L KCl, 0.5 mmol/L phenylmethylsulfonyl fluoride, 0.5 mmol/L dithiothreitol plus protease inhibitor cocktail (Roche)] for 15 min. Cells were then lysed with 12.5 μl 10% Nonidet P-40. The homogenate was centrifuged (13,000*g*, 30 s), and supernatants containing the cytoplasmic extracts were stored at −80°C. The nuclear pellet was resuspended in 100-μl ice-cold hypertonic extraction buffer [10 mmol/L HEPES (pH 7.9), 0.42 M NaCl, 1.5 mmol/L $MgCl_2$, 10 mmol/L KCl, 0.5 mmol/L phenylmethylsulfonyl fluoride, 1 mmol/L dithiothreitol plus protease inhibitors]. After 40 min of intermittent mixing, extracts were centrifuged (13,000*g*, 10 min, 4°C), and supernatants containing nuclear proteins were secured. The protein content was measured by the Bradford method [18–20].

2.8. NFκB-p65 enzyme-linked immunosorbent assay for determination of NFκB activity

A total of 10 μg of nuclear extracts was used to determine the NFκB DNA-binding activity [NFκB p65 enzyme-linked immunosorbent assay (ELISA) kit, Stressgen/Assays designs] per manufacturer's protocols. This ELISA-based chemiluminescent detection method rapidly detects activated NFκB complex binding (p65 detection) to a plate-adhered NFκB consensus oligonucleotide sequence. Kit-provided nuclear extracts prepared from TNF-stimulated Hela cells were used as a positive control for NFκB activation. To demonstrate assay specificity, a 50-fold excess of an NFκB consensus oligonucleotide was used as competitor to block NFκB binding. In addition, a mutated consensus NFκB oligonucleotide (which does not bind NFκB) is provided for determination of binding reactions' specificity [21].

2.9. Western blotting

Proteins (20 μg) were separated by sodium dodecyl sulfate polyacrylamide gel electrophoresis on 10% (wt/vol) acrylamide and 0.275% (wt/vol) bisacrylamide gels and electrotransferred onto nitrocellulose membranes. Membranes were incubated in TBS-T [20 mmol/L Tris–HCl, pH 7.5, 137 mmol/L NaCl, 0.05% (vol/vol) Tween 20] containing 1% (wt/vol) nonfat milk powder for 1 h at room temperature. Subsequently, the membranes were incubated for 12 h with the appropriate primary antibody (dilution range 1:500–1:1000), rinsed with TBS-T and exposed to horseradish-peroxidase-linked anti-IgG antibodies for 2 h at room temperature. Chemiluminescent bands were detected using X-ray films, and densitometry analyses were performed using Image-J software.

2.10. Mitochondria membrane potential (JC-1 assay)

For determination of the mitochondrial membrane potential (MMP), treated cells (5×10^5) were incubated for 30 min at 37°C with the lipophilic cationic probe JC-1 (5,5′,6,6′-tetrachloro-1,1′,3,3′ tetraethylbenzimidazolcarbocyanine iodide, 2 μg/ml). Afterward, JC-1-loaded cells were centrifuged and washed once with PBS. Cells were transferred to a 96-well plate and assayed in a fluorescence plate reader with the following settings: excitation at 485 nm, emission at 540 and 590 nm and cutoff at 530 nm (SpectraMax M2, Molecular Devices, USA). $\Delta\Psi m$ was calculated using the ratio of 590 nm (J-aggregates)/540 nm (monomeric form) [22].

2.11. Clonogenic potential

Exponentially growing cells (1×10^6) were plated in petri plates overnight and then incubated for 36 h with either vehicle or curcumin. After treatments, the medium containing curcumin was replaced by a curcumin-free medium, and remaining cells were maintained for additional 24 h to growth. Survival cells were gently washed and

Table 1
IC_{50} levels of curcumin in a panel of GBMs and astrocytes

Cell lines	Curcumin IC_{50} (μM)
U138MG	29±5[a]
C6	25±4[a]
U87	19±7[a]
U373	21±3[a]
Astrocytes	135±12

Legend: Cells (U138MG, U87, C6, U373 and astrocytes) were treated for 36 h with different concentrations of curcumin (1–150 μM), and cell viability was determined by MTT assay. Experiments were repeated three times (n=3) in triplicate, and data were expressed in mean±S.D.

[a] Different from astrocytic IC_{50} value (P<.05, t test).

Table 2
LDH release and cellular viability in curcumin-treated C6 and astrocytes

Curcumin (μM)	C6 cells		Astrocytes	
	Viability (MTT, %)	LDH (%)	Viability (MTT, %)	LDH (%)
0	100±3	100±14	100±9	100±11
7.5	90±2[a]	113±21	101±3	102±13
15	78±5[b]	120±36	103±4	98±19
25	67±2[b]	276±92[a]	102±17	89±9
50	28±3[b]	907±105[b]	108±13	121±13
100	10±5[b]	1251±57[b]	110±15	115±33
120	3±1[b]	1290±154[a]	81±9[a]	169±14[a]

Legend: Cells were treated with curcumin for 36 h; medium was collected for LDH activity determination, and cells were used for viability estimation by MTT assay. Experiments were repeated three times (n=3) in triplicate, and data were expressed in mean±S.D.
[a] Different from untreated cells.
[b] Different from untreated cells and from the immediately lower curcumin concentration (P<.05, ANOVA).

trypsinized, and viability was assessed by trypan blue staining. Viable cells (10^4 cells) were replated in six-well plates and maintained for additional 6 days in complete culture medium. Cell growth was estimated by colony counting followed by MTT assay [21]. The percentage of colony forming efficiency was calculated in relation to values of untreated cells.

2.12. Soft agar colony assay

Cells (1×10^5) were resuspended in 2 ml DMEM supplemented with 15% FBS and mixed with 1 ml of 1.6% agarose (final conditions: 0.53% agarose and 10% FBS) at 37°C. Cell suspensions were placed on top of a base layer comprised of 2 ml of DMEM with 10% FBS and 0.8% agarose in each well of a six-well plate. Cells were then covered with 2 ml of complete media, and after 3 days, a new medium containing curcumin was added. Medium containing treatments or vehicle was replaced every 72 h. At the end of 9 days, MTT (1 mg/ml) was added to the cultures, and the number of colonies was scored using a microscope [21].

2.13. Migration assay

The monolayer of confluent C6 and U138MG cells was pretreated for 12 h with curcumin and subsequently scratched with a 200 μl pipette tip to create a wound. Cells were washed twice with PBS to remove floating cells and then incubated in DMEM with 2% FBS plus treatments. Cells were incubated for additional 16–18 h, and the rate of wound closure was investigated through photographs (100×) taken at final time points. Migration of treated cells was compared to untreated cells and expressed as percentage [23].

2.14. Proliferation assay

For proliferation assay, 24-well-plated cells were treated at 50%–60% confluence during 72 h (chronic exposure) with curcumin inhibitors. After treatments, cells were fixed in ethanol:acetone (1:1) for 5 min followed by PBS washing (three times). Fixed cells were stained with trypan blue 0.4% (Sigma, CA, USA) for 30 min and washed three times with PBS. Trypan-stained cells were lysed with 1 N NaOH for 5 min. Afterward, equal volume of distillated water was added, and trypan blue color was estimated in spectrophotometer at 595 nm [24]. Sample absorbance was compared to controls and expressed as percentage of untreated cells.

2.15. Preclinical study: glioma in vivo experiments

2.15.1. Implantation

In vivo model of rat C6 glioma was carried out as previously described by Takano et al. [25] and validated in our laboratory [26,27]. Exponentially growing C6 cells were trypsinized, washed once in DMEM, spun down and resuspended at 10^6 cells/3 μl DMEM. Cells were injected using a 5-μl Hamilton microsyringe coupled in the infusion pump (1 μl/min) at a depth of 6.0 mm into the right striatum (coordinates with regard to bregma: 0.5 mm posterior and 3.0 mm lateral) of adult male Wistar rats (8 weeks old, 220–260 g) previously anesthetized by intraperitoneal (ip) administration of

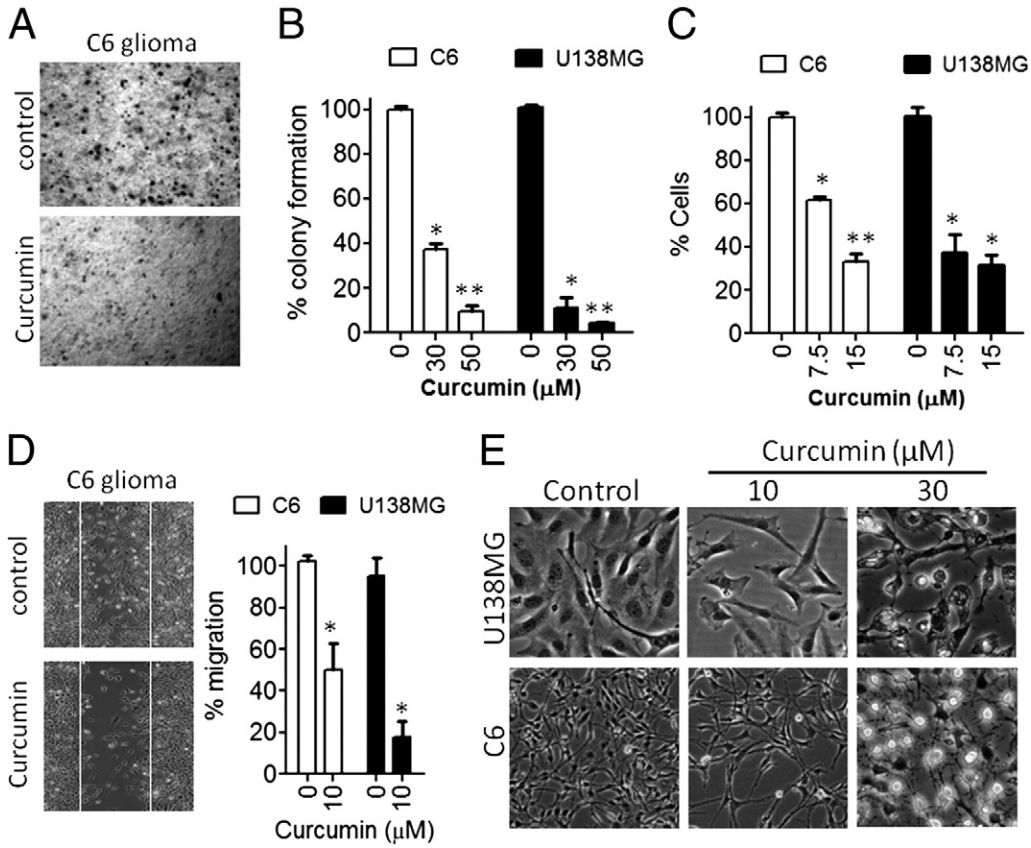

Fig. 1. Curcumin inhibits GBM cells growth. (A) Curcumin 30 μM inhibits the growth of C6 cells in soft agar. (B) Short-term incubation with curcumin reduces clonogenic potential of C6 and U138MG cells. (C) Effect of subtoxic concentrations of curcumin on proliferation of C6 and U138MG cell lines. Cells were treated for 72 h with 7.5 or 15 μM curcumin, fixed and stained with trypan blue for estimation of cell density. Cell morphology was monitored by light microscopy. *Different from untreated cells; **different from the immediately lower curcumin concentration, P<.05, ANOVA. (D) Subtoxic concentrations of curcumin (10 μM) decrease U138MG and C6 cells migration. *Different from untreated cells, P<.05, t test. (E) Representative microphotographs (20×) showing the effect of cytotoxic (30 μM) and subapoptotic (10 μM) concentrations of curcumin on morphology of U138MG and C6 cells. All experiments were repeated at least four times (n=4).

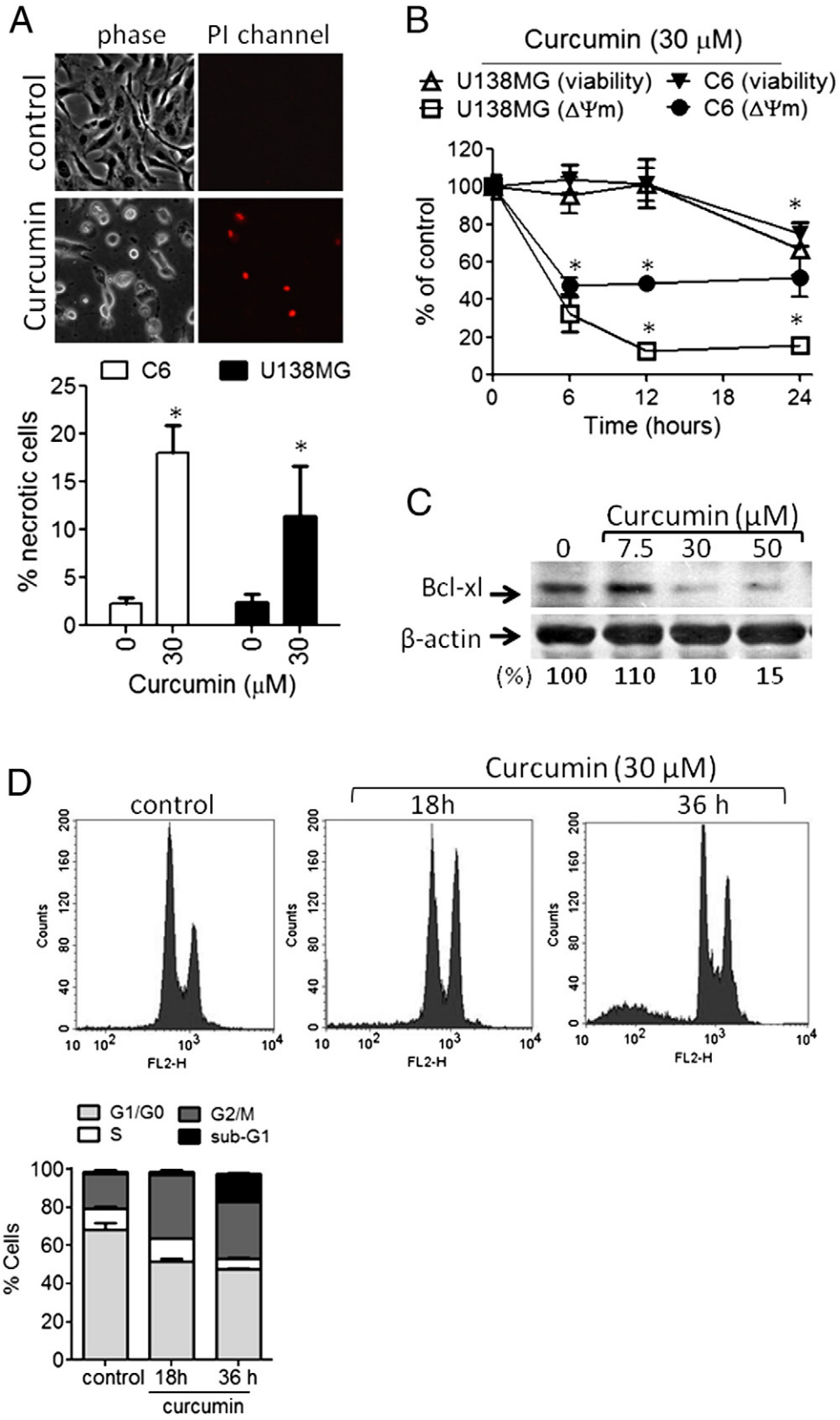

Fig. 2. Curcumin induces mitochondrial dysfunction and programmed cell death in GBMs. (A) Propidium iodide incorporation in U138MG cells. After 36-h treatment with 30 μM curcumin, cells were incubated with PI diluted in culture medium. Fluorescence and phase contrast microphotographs were taken (20×). The percentage of PI-stained cells was quantified. *Different from untreated cells, $P<.05$, t test. (B) Time course effect of curcumin on MMP was co-evaluated with PI incorporation for determination of cell membrane integrity. U138MG cells were treated for different times and trypsinized, and different aliquots were collected for JC-1 or PI incorporation assays. *Different from untreated cells, $P<.05$, t test. (C) Curcumin decreases bcl-xL protein immunocontent as assessed by Western blotting in total cell extracts of 12-h-treated U138MG cells. (D) Flow cytometry for determination of cell cycle distribution (sub-G1, G1/G0, S and G2/M) in untreated and 30 μM curcumin-treated (18–36 h) U138MG cells. All experiments were repeated at least three times ($n=3$).

ketamine/xylazine. The number of animals for 95% confidence was statistically calculated in agreement with our previously determined standard deviations (S) and means (μ) of tumor size for the *in vivo* model of glioma [26]. Data/legends: A=DMSO-treated rats (control); B=alkylation-agent-treated rats (control for antiglioma activity); statistical parameters: μ_A=73 mm^3; μ_B=27 mm^3; S_A=13 mm^3; S_B=37 mm^3; α=0.05, power=1−β=0.9; β=0.1; t_α=2.101; u_β=1,734; n_0=10. Formula: $n=((S_A)^2+(S_b)^2)/(\mu_A-\mu_b)^2\times(t_\alpha+u_\beta)^2$; n=11 rats/group. All procedures used in the present study followed the "Principles of Laboratory Animal Care" of the National Institutes of Health and were approved by the Ethical Committee of the Hospital de Clinicas de Porto Alegre.

2.15.2. Treatments

Ten days after glioma implantation, animals were divided into two groups (n=11 per group) as follows: (a) DMSO/vehicle-treated group and (b) curcumin-treated group (50 mg/kg/day curcumin solubilized in sterile DMSO). The formulations were administered ip for 10 consecutive days.

2.15.3. Analysis

After 20 days (10 days for glioma implantation+10 days for treatments), rats were anesthetized and decapitated. The brain was removed, sectioned and fixed with 10% paraformaldehyde. Cerebellum, liver and kidney were also removed and frozen at −80°C for biochemical analysis. Blood samples were collected for determination of glucose, total cholesterol, creatinine, alkaline phosphatase, alanine aminotransferase (ALT) and aspartate aminotransferase (AST) activity in serum, which were used as markers of metabolic and tissue toxicity. These experiments were performed in a LabMax 240 analyzer (Labtest Diagnostica, Brazil). Hematological parameters were evaluated in a Sysmex KX-21-N hematologic analyzer (Sysmex, Lille, France). The oxidative stress parameters TBARS (lipoperoxidation), protein sulfhydryl and carbonyl groups, catalase, superoxide dismutase and glutathione *S*-transferase (GST) activity were evaluated in cerebellum, liver and kidney in agreement with our previously described protocols [28].

For tumor volume quantification, three hematoxylin and eosin (H&E) coronal sections (2–3 μm thick, paraffin embedded) from each animal were analyzed. Images were captured using a digital camera connected to a microscope (Nikon Eclipse TE300), and the tumor area (mm^2) was determined using Image Tool Software. The total volume (mm^3) of the tumor was computed by the multiplication of the slice sections and by summing the segmented areas [26,27]. In animals with detectable tumor mass, histopathological parameters were evaluated by two expert pathologists.

2.16. Statistical analysis

The statistical significance among three or more groups was assessed by one-way analysis of variance (ANOVA) followed by Tukey's test. The statistical significance between DMSO-treated and curcumin-treated groups and other two-group analyses were carried out by means of unpaired Student's t test (Prism GraphPad Software, San Diego, CA, USA). For qualitative data (Table 4 experiments), Z-test for two proportions and Fisher's Exact Test were chosen. Significant differences among groups were calculated at P<.05.

3. Results

3.1. Curcumin inhibits proliferation and induces cell death in GBMs but not in astrocytes

First, we examined the effect of curcumin on viability of GBMs by treating a panel of GBM cell lines (C6, U138MG, U87, U373) with different concentrations of curcumin for 36 h. At the end of incubation, MTT assays were carried out. In parallel, primary astrocytes cultures were used as a nontransformed model of glial cells in order to test the selectivity of curcumin. Curcumin markedly decreased the viability of the four GBM cells lines (IC_{50} range=19–28 μM), whereas astrocytes were much less sensitive to curcumin treatment (IC_{50}=135 μM) as assessed by MTT (Table 1). Curcumin also caused a dose-dependent release of LDH into culture medium of GBMs, indicating losses in cell membrane integrity. Curcumin-induced LDH release was associated with decreases in cell viability as assessed by MTT (Table 2). In astrocytes, toxicity only was observed at high curcumin concentrations (120 μM). Taken together, these data suggest that the cytotoxic effects of curcumin selectively targeted GBMs (Table 2). For further experiments, we used ~IC_{50} concentrations of curcumin, and the C6 and U138MG cell lines since (a) they have different patterns of p53 mutations, (b) curcumin mechanisms were not determined in these cell lines and (c) C6 cells were used in *in vivo* experiments.

Curcumin-induced growth inhibition was independent on cell anchorage to extracellular matrix as evaluated by soft agar growth experiments (Fig. 1A). In addition, results from clonogenic survival assays showed that curcumin treatment (24 h) followed by 6-day washout significantly decreased the clonogenic proliferation in GBMs, suggesting that curcumin effects were prolonged and persisted after drug withdrawal (Fig. 1B). Significant morphological alterations and cell detachment were observed in 30 μM curcumin-treated cells (Fig. 1E). At low concentrations (≤15 μM), curcumin caused decreases in cell viability and cell density (Table 2 and Fig.

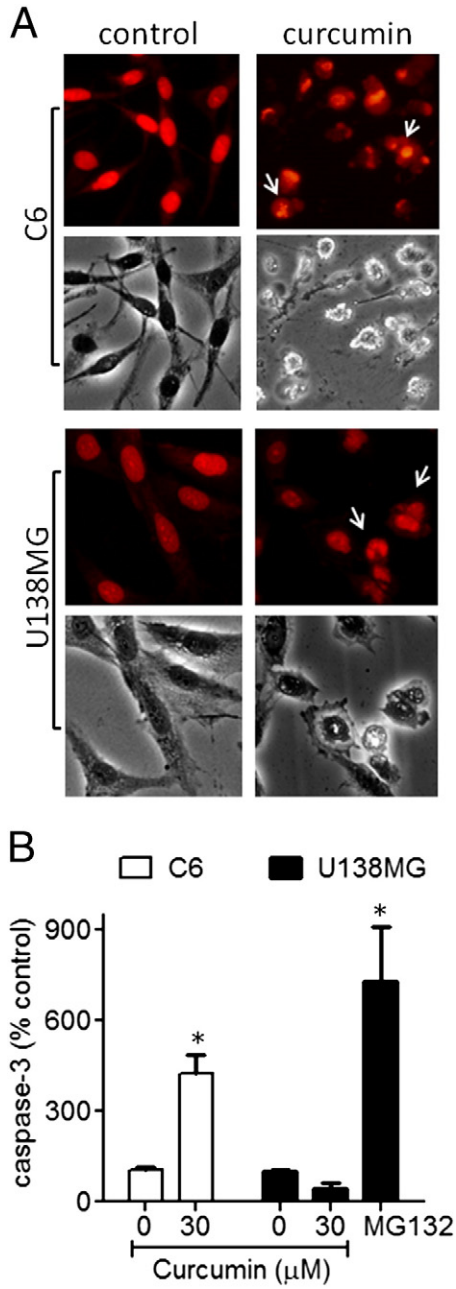

Fig. 3. Curcumin promotes chromatin condensation and modulates caspase-3 in GBMs. (A) Representative fluorescence and phase contrast microphotographs (40×) showing the effect of 30 μM curcumin (36-h treatment) on condensation of chromatin and formation of apoptotic bodies in C6 and U138MG cells. (B) Caspase-3 activity after 36-h treatment with 30 μM curcumin in C6 and U138MG. *Different from untreated cells, P<.05, t test, n=4.

1E), but induced neither LDH release nor alterations in cell morphology (Fig. 1E), indicating a cytostatic/antiproliferative effect of curcumin at noncytotoxic concentrations. Therefore, we decided to test whether a long-term exposure to subtoxic curcumin could decrease cell proliferation. Curcumin (7.5 and 15 μM) decreased cell proliferation by up to 73%±12% after 72-h exposure when compared

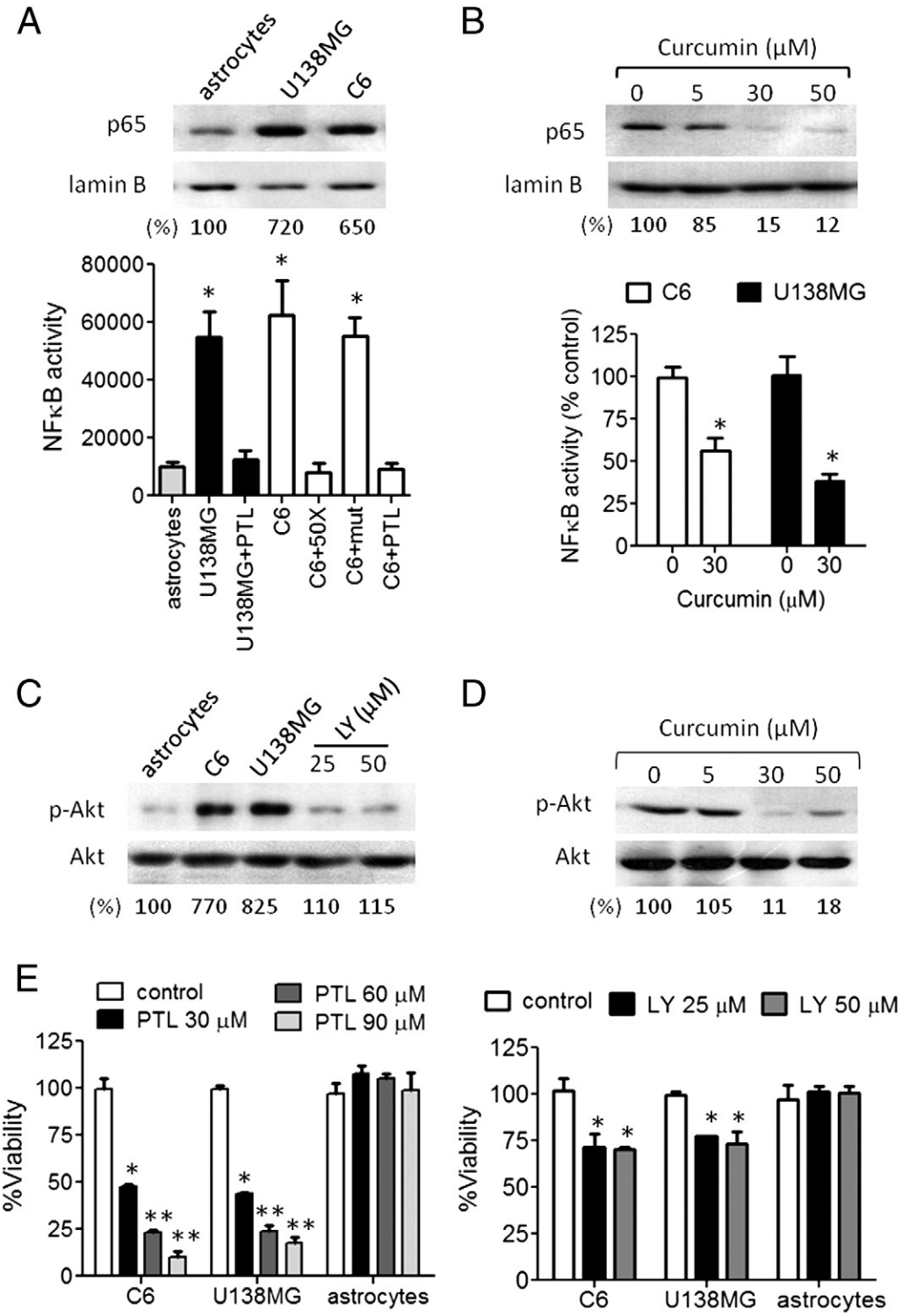

Fig. 4. Curcumin suppresses activation of NFkappaB and PI3K/Akt in GBMs. (A) Constitutive NFkappaB activation and nuclear levels of p65 in C6, U138MG and astrocytes. Cells were maintained in equal basal conditions (complete culture medium for 48 h), and nuclear extracts were isolated for detection of NFkappaB activity (ELISA kit) and p65 immunocontent (Western blotting). Lamin B was used as loading control for nuclear extracts. *Different from astrocytes, $P<.05$, ANOVA. (B) Curcumin inhibits NFkappaB DNA-binding activity and p65 translocation in GBM. The ELISA assays and Western blots were carried out in nuclear extracts isolated from 6-h-treated U138MG cells. [a]Different from untreated cells, $P<.05$, t test. (C) Constitutive PI3K/Akt pathway activation in C6, U138MG and astrocytes. Cells were maintained in basal conditions (above cited), and Western blotting for p-Akt and total-Akt forms was performed in total extracts. Beta-actin was used as loading control (not shown). (D) Curcumin inhibits Akt phosphorylation. U138MG cells were treated for 6 h with 5 to 60 μM curcumin followed by Western blotting for p-Akt protein detection. (E) The MTT assays showing the effect of different concentrations of PTL or LY294002 (LY) on viability of GBM cell lines and astrocytes. *Different from untreated cells; **different from untreated and from the immediately lower concentration of PTL or LY, $P<.05$, ANOVA, $n=3$.

Table 3
Curcumin synergizes with classical chemotherapy

Treatments	Viability (MTT, %)	
	U138MG	C6
Untreated	100±5.7	100±2.1
Cisplatin	63±6.0[a]	42±3.3[a]
Cisplatin+curcumin 10 μM	46±5.9[b]	29±2.4[b]
Cisplatin+curcumin 25 μM	30±3.2[b]	10±4.2[b]
Doxorubicin	66±2.0[a]	73±4.2[a]
Doxorubicin+curcumin 10 μM	48±3.3[b]	61±3.0[b]
Doxorubicin+curcumin 25 μM	36±4.6[b]	46±5.4[b]
Curcumin 10 μM	76±1.2[a]	88±5.1[a]
Curcumin 25 μM	55±5.0[a]	75±7.3[a]

Legend: U138MG and C6 cells lines were treated with different concentrations of curcumin, followed by exposure to cisplatin or doxorubicin for 48 h. Data were collected from three independent experiments (n=3) performed in triplicate.
[a] Different from untreated cells.
[b] Different from its respective cisplatin or doxorubicin monotreatment, P<.05, ANOVA.

to untreated cells (Fig. 1B). In addition, subtoxic curcumin (10 μM) also inhibited the migration of both C6 and U138MG cells as assessed by scratching assay (Fig. 1C).

3.2. Curcumin induces mitochondrial dysfunction, cell cycle arrest and apoptosis in GBMs

At the end of 36-h incubation, we observed significant morphological alterations in curcumin-treated cells, which were accompanied by PI uptake (Fig. 2A). However, PI uptake did not occur in all cells with changes in morphology, suggesting that morphological alterations preceded the losses in cell membrane permeability (Fig. 2A). These events suggest a programmed mechanism of cell death. Curcumin caused an early collapse in the MMP ($\Delta\Psi$m, Fig. 2B) and decreased the immunocontent of the cytoprotective mitochondrial protein bcl-xL (Fig. 2C). These events preceded curcumin-induced losses in plasmatic membrane integrity (PI incorporation assays, Fig. 2B). Curcumin-induced decreases in MMP and bcl-xl protein were clearly observed at 12-h treatment, whereas PI uptake only increased at later time points (24 h). By flow cytometry, we determined that curcumin caused cell arrest in the G2/M phase of the cell cycle at 18-h treatment, which cumulated in formation of a significant population of hypodiploid (sub-G1) cells at 36 h, indicating that G2/M arrest preceded apoptosis in curcumin-treated cells (Fig. 2D). Staining of chromatin with PI showed that curcumin induced chromatin condensation and formation of apoptotic bodies in GBMs after 36-h incubation (Fig. 3A). Activation of the executor caspase-3 was detectable in C6 cells but not in the p53-mutant U138MG (Fig. 3B). The proteasome inhibitor MG132 was used as a positive control for caspase-3 activation in order to confirm the noneffect of curcumin on caspase-3 in U138MG.

3.3. Curcumin inhibits PI3K/Akt and NFkappaB survival pathways in GBMs

NFkappaB and PI3K/Akt are considered as two important GBMs survival pathways [29,30]. NFkappaB was found up-regulated in the GBM cell lines (six- to sevenfold) compared to astrocytes as detected by ELISA assays for NFkappaB activity and Western blotting for nuclear p65 protein (Fig. 4A). Treatment with curcumin for 6 h decreased both NFkappaB activity and nuclear accumulation of p65 (Fig. 4B). Taking into account that curcumin also decreased the NFkappaB-regulated protein bcl-xl (Fig. 3B), these results indicate that curcumin inhibits NFkappaB signaling in GBMs. The ELISA assay specificity was confirmed by incubation of nuclear extracts with kit-provided 50× unlabeled oligonucleotides, which inhibited completely NFkappaB basal binding (C6+50× lane). In addition, mutant oligonucleotides did not alter NFkappaB activity, confirming the specificity of the binding reactions (C6+mut lane). The pharmacological NFkappaB inhibitor PTL was used as a control for NFkappaB inhibition (Fig. 4A); LPS was used as a control for NFkappaB activation (not shown).

PI3K/Akt pathway also was found up-regulated (seven- to eightfold increase) in C6 and U138MG cell lines compared to astrocytes (Fig. 4C). Curcumin inhibited about 80% the constitutive activation of the PI3K/Akt pathway as detected from levels of the phosphorylated forms of Akt, a surrogate to evaluate PI3K/Akt pathway activation in GBMs. Total forms of Akt were not altered, indicating that the protein was modulated in the posttranslational level (Fig. 4D). Controls for specific PI3K/Akt inhibition were performed by incubating cells with LY294002 (see Fig. 4C, LY lanes).

To evaluate/confirm whether NFkappaB and PI3K/Akt pathways, which were blocked by curcumin, play a role in survival of GBMs, we treated C6, U138MG and astrocytes with inhibitors of NFkappaB (PTL) and PI3K/Akt (LY294002) for 36 h; MTT assays were performed. NFkappaB and PI3K inhibitors decreased the cellular viability in GBM cell lines but exerted no effects on astrocytic viability (Fig. 4E).

3.4. Curcumin synergizes with clinically utilized anticancer drugs

Adjuvant therapy has the therapeutic advantage of potentiating the effect of classical anticancer drugs, thereby decreasing the frequently observed systemic side effects and damage to healthy tissues [31]. To explore the potential of curcumin as a chemotherapeutic adjuvant, we pretreated U138MG and C6 cells with subapoptotic (12-h pretreatment followed by 48-h coincubation) or apoptotic (12-h curcumin pretreatment, washout and subsequent 48-h incubation with anticancer drugs alone) concentrations of curcumin either alone or in combination with the alkylation agent cisplatin (5 μM) or the topoisomerase inhibitor doxorubicin (2.5 μM). The MTT assays showed that curcumin synergized with the anticancer drugs in both apoptotic and subapoptotic concentrations, potentiating the effects of the cisplatin and doxorubicin in the two tested cell lines (Table 3).

3.5. Curcumin inhibits GBM growth in vivo

In order to determine whether curcumin antiglioma potential *in vitro* could be achieved *in vivo*, we treated C6-implanted Wistar rats with 50 mg/kg/day curcumin, ip, from the 10th to the 20th day after glioma implantation. This *in vivo* model is one of the most useful tools to evaluate the pharmacologic potential of a drug in the growth of gliomas since tumor cells are induced to grow in the brain of immune-competent animals, thus simulating much of the *in vivo* conditions of GBMs [25–27]. Of the curcumin-treated rats, only 7/11 (63%) developed detectable tumors vs. 11/11 (100%) in the DMSO-treated

Table 4
Histological analysis of H&E-stained brain sections of glioma-implanted rats

Histology	DMSO	Curcumin	Z-value/confidence
Rats with tumor development	11/11 (100%)	7/11 (64%)	1.66[a]/96%[a]
Coagulative necrosis	10/11 (91%)	5/7 (71%)	0.43/67%
Intratumoral hemorrhage	9/11 (82%)	3/7 (43%)	1.2/88%
Lymphocytic infiltration	9/11 (82%)	4/7 (57%)	0.6/72%
Peritumoral edema	9/11 (82%)	5/7 (71%)	−0.065/47%
Peripheral pseudopalisading	6/11 (54%)	5/7 (71%)	−0.065/47%

Legend: The proportion of animals that developed a defined tumor mass as evaluated by H&E analysis. The histological variables (coagulative necrosis, intratumoral hemorrhage, lymphocytic infiltration, peritumoral edema, peripheric pseudopalisading) were regarded as present or absent.
[a] Different from DMSO-treated rats at α>95 % confidence level (DMSO vs. curcumin , Z-test).

group (Table 4) as evaluated by histochemistry. Quantification of tumor volume was carried out exclusively in animals presenting a body mass that could be quantified. In the curcumin-treated rats with detectable tumors (seven rats), we observed decreases in tumor volume in five of seven (71%) animals, whereas all DMSO-treated rats (11/11) presented marked tumor masses (Fig. 5A). Results showed

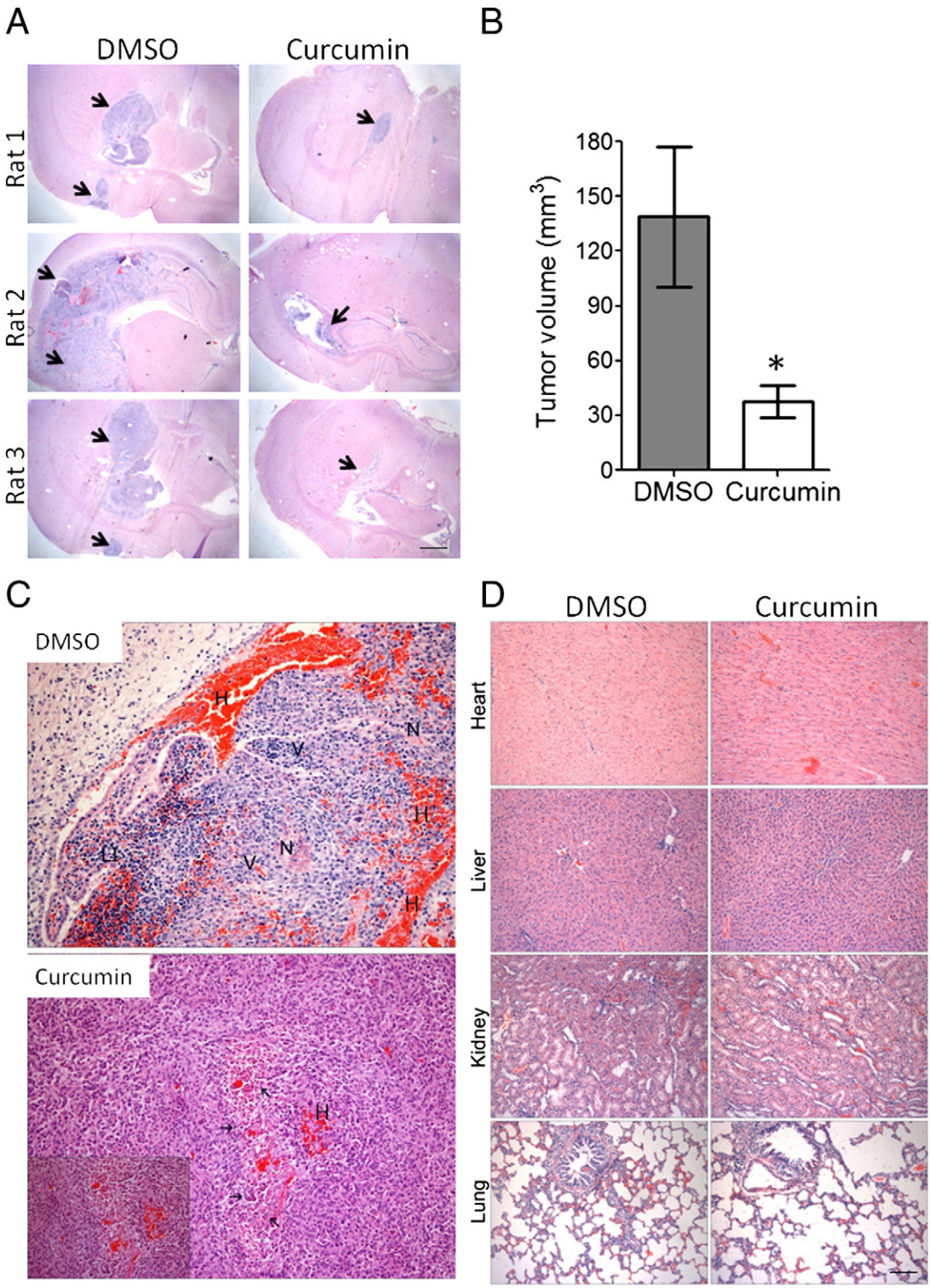

Fig. 5. Curcumin inhibits GBM growth *in vivo*. Animals were treated, and samples were analyzed as described in Materials and Methods. (A) Representative H&E-stained brain coronal sections of C6 tumors (arrows) of three representative animals of the control group (DMSO treated) and of the curcumin-treated group. Scale bars=1 mm. (B) Tumor volume (mm^3) quantification of implanted gliomas. *Different from DMSO-treated controls, $P<.05$, DMSO vs. curcumin , *t* test, mean±S.D. (C) Histopathology of C6 tumors. Legends: DMSO-treated group: (N) necrosis, (H) hemorrhages, (V) vascular proliferation, (LI) lymphocytic infiltration; curcumin-treated group: pathological characteristics of tumor in involution; arrows: apoptotic cells; (H) hemorrhages. Magnification 20×; insert 40×. (D) Representative microphotographs showing H&E-stained sections of liver, lung, kidney and heart of DMSO-treated and curcumin-treated glioma-implanted rats; magnification 10×.

Table 5
Hematological parameters and tissue damage serum markers in curcumin- and DMSO-treated C6 implanted rats

	DMSO	Curcumin
White blood cells ($\times 10^3$/mm^3)	4.8±1.2	4.92±1.6
Red blood cells ($\times 10^6$/mm^3)	7.38±0.7	7.37±0.6
Hematocrit (%)	40±4	41±3
Platelets ($\times$103/mm^3)	872±67	850±140
RDW (%)	14±0.4	15.1±0.5
Lymphocytes (%)	74.3±2.5	75.2±5.5
Granulocytes (%)	15.3±3.2	15.7±3.6
Monocytes (%)	10.3±2.4	9.1±2.1
AST (U/L)	186±30	194±35
ALT (U/L)	82±9	71±5
Alkaline phosphatase (U/L)	240±61	166±78
Creatinine (mg/dl)	0.5±0.05	0.49±0.1
Glucose (mg/dl)	161±33	143±35
Total cholesterol (mg/dl)	41±3	44±8

that the animals treated with curcumin displayed a significant reduction in tumor size (mean±S.D.: 37±9 mm^3, n=7) compared to the DMSO-treated (mean±S.D.=138±37 mm^3, n=11) group (Fig. 5B). Representative H&E-stained tumor sections are shown in Fig. 5A (arrows indicate tumor areas). It is important to cite that, of the 11 tumor-implanted animals in the DMSO group, two animals presented losses in body weight and motor impairment and died between the 18th and 19th day of experiment due to glioma complications.

Besides reducing tumors size, curcumin increased the number of apoptotic cells in tumors as detected by microscopic analysis of H&E-stained brain sections (Fig. 5C, arrows show apoptotic areas). On the other hand, although the percentage/proportion of animals with intratumoral hemorrhage (curcumin: 3/7 vs. DMSO: 9/11) and lymphocytic infiltration (curcumin: 4/7 vs. DMSO: 9/11) appeared to be lower in curcumin-treated rats, the proportions, which were based on qualitative analysis of "presence or absence" of the alterations, were not statistically different from DMSO-treated rats (Table 4). However, the hemorrhagic areas in curcumin-treated rats were clearly reduced when compared to DMSO-treated rats (Fig. 5C, red regions indicate intratumoral hemorrhage, H).

Importantly, curcumin neither altered hematological parameters (leukogram and hemogram) nor exerted tissue or metabolic toxicity as evaluated from determination of ALT, AST (liver damage marker), creatinine (kidney damage marker), alkaline phosphatase (pancreas, liver and bone unspecific damage markers), glucose and total cholesterol (Table 5). Means in curcumin-treated group did not differ from means in DMSO-treated rats (t test; P>.05). In addition, curcumin did not alter oxidative stress parameters in cerebellum, liver and kidney as evaluated from quantification of TBARS, protein carbonyl, sulfhydryl and antioxidant enzymes activity (Table 6). Microscopic investigation of liver, kidney, lungs and hearts by H&E analysis also demonstrated absence of tissue toxicity in curcumin-treated rats. Representative histologies of liver, kidney, lungs and heart tissues in curcumin- and DMSO-treated rats are shown in Fig. 5D.

4. Discussion

The present study showed a potent and selective cytotoxic effect of the dietary compound curcumin in a panel of GBM cell lines and in glioma implants. Curcumin effect occurred in both adhered and agar-growing GBMs, evidencing an anchorage-independent mechanism. In addition, the antiglioma activity of curcumin was prolonged and persisted for several days after drug withdrawal as assessed by clonogenic assays. Besides cell death induction at cytotoxic levels, low concentrations of curcumin decreased proliferation and migration and synergized with classical anticancer drugs, suggesting that subtoxic concentrations of curcumin also could be taken for therapeutic advantage.

Curcumin appeared to act irrespective of the p53 or PTEN mutational status of the cells, since U138MG, U373 (PTEN mutated/p53 mutated), U87 (PTEN mutates/p53 wild-type) and C6 (PTEN wild-type/p53 wild-type), which possess different mutations, were sensitive to curcumin. Defects in apoptotic signaling pathways as p53 mutations and caspases down-regulation promote chemoresistance and limit the effectiveness of chemotherapeutics [32–37]. Curcumin stimulated effector caspase-3 in C6 but not in the p53-mutant U138MG, indicating that curcumin can activate either caspase-dependent or caspase-independent cell death pathways depending on the cell line. In agreement, prior studies reported that curcumin exerts caspases, calpains and p53-independent cell death via inhibition of NFkappaB in the p53-mutated T98G cell line [21]. Thus, curcumin's ability to induce caspase/p53-independent cell death circumvents two frequent aberrations that contribute to GBM resistance.

Curcumin suppressed NFkappaB and PI3K/Akt, which are two pivotal survival pathways in GBMs [38–44]. Mutations in the tensin homolog PTEN, a negative regulator of PI3K, leads to losses in PTEN activity and to constitutive activation of the PI3K/Akt pathway in most of gliomas [40,45]. On the other hand, NFkappaB up-regulation has been attributed to cytokine overproduction, deregulation of PI3K/Akt [40], RIP-1 [41] and EGFR pathways [42]. Aberrant activation of NFkappaB has been reported in GBM biopsies, and focal necrosis formation, invasive phenotypes [43] and resistance to O^6 alkylating agents [39] paralleled the activity of this pathway in these tumors. In high-grade astrocytoma and GBM, a positive correlation between phospho-Akt, NFκB activation and glioma progression was observed [43]. Therefore, PI3K/Akt and NFkappaB pathways become important therapeutic targets for these tumors. We found a constitutive activation of PI3K/Akt and NFkappaB in GBM cell lines but not in astrocytes. Inhibition of NFkappaB and PI3K/Akt with the pharmacological inhibitors LY294002 and PTL selectively decreased cellular viability in GBMs, confirming the role of these pathways in GBM cells survival. Taking into account the aforementioned, the mechanisms whereby curcumin is protective in normal cells, yet death inducing in tumor cells, could be explained by its ability to block survival pathways that are constitutively active in cancer but not in healthy cells, such as PI3K/Akt and NFkappaB [31,43,44]. Although markedly

Table 6
Oxidative stress markers in liver, kidney and cerebellum of C6 implanted rats after 10 days of DMSO or curcumin treatment

	DMSO	Curcumin
Liver		
TBARS (nmol/mg protein)	0.092±0.031	0.078±0.026
Sulfhydryl (μmol/mg protein)	76.1±3.9	78.6±1.0
Carbonyl (nmol/mg protein)	1.1±0.3	0.77±0.35
Catalase (U/mg protein)	113±14.5	107±9.1
SOD (U/mg protein)	48.4±2.2	48.9±1.9
GST (U/mg protein)	2.70±0.12	2.68±0.11
Kidney		
TBARS (nmol/mg protein)	0.64±0.05	0.59±0.04
Sulfhydryl (μmol/mg protein)	73.8±1.2	71.5±2.0
Carbonyl (nmol/mg protein)	1.47±0.6	1.15±0.25
Catalase (U/mg protein)	29.9±1.7	27.6±0.8
SOD (U/mg protein)	62.8±1.8	63.1±1.4
GST (U/mg protein)	1.1±0.02	1.2±0.08
Cerebellum		
TBARS (nmol/mg protein)	0.50±0.04	0.47±0.03
Sulfhydryl (μmol/mg protein)	79.6±3.4	78±1.8
Carbonyl (nmol/mg protein)	1.2±0.31	0.95±0.4
Catalase (U/mg protein)	2.25±0.11	2.32±0.12
SOD (U/mg protein)	35.5±0.84	33.7±0.63
GST (U/mg protein)	2.08±0.13	2.23±0.12

cytotoxic to GBMs, curcumin spared nontransformed cells, except for a minor reduction in astrocytic viability after 100 μM, which may be restricted to proliferating astrocytes in culture; a property not shared *in vivo* [21]. The arrest in the G2/M phase as an early step of the apoptotic mechanism also could contribute to curcumin selectivity, since cancer cells are in constant cell cycle progression through S to G2/M phase, in contrast to nonproliferative cells. Previous studies showed that curcumin seems unlikely to affect normal brain function and, in fact, is neuroprotective in animal models of ischemic stroke and Alzheimer's disease [46–49].

Despite aggressive neurosurgery and chemotherapy, GBMs frequently exhibit chemoresistance [39,48–51]. Identifying novel strategies to overcome drug resistance may aid in the development of improved therapeutics. In C6 and U138MG, curcumin decreased the nuclear activity of NFkappaB, causing reduction of the bcl-xl protein immunocontent, which is a classical NFkappaB-regulated mitochondrial antiapoptotic protein. Moreover, curcumin synergized with the chemotherapeutics doxorubicin and cisplatin to cause toxicity in GBMs. This implies that curcumin may be a potential adjuvant by decreasing the antiapoptotic threshold, leading to sensitization to anticancer drugs' apoptotic stimuli. Previous studies have shown that curcumin decreases the expression of NFkappaB-regulated genes as bcl-xL, XIAP, cIAPs and survivin in T98G cells, which contribute to chemoresistance [21,52,53]. We previously reported that down-regulation of NFkappaB by BAY117082 and MG132 leads to mitochondrial dysfunction due to decreases in bcl-xL and SOD2 in leukemic cell lines [18]. Selective bcl-xL knockdown rendered U87 and NS008 GBM cells apoptosis [53], suggesting that bcl-xL down-regulation may induce mitochondrial dysfunction that ultimately results in cytotoxicity. Here, curcumin decreased bcl-xL and caused mitochondrial depolarization, which preceded the losses in cell membrane integrity, suggesting the mitochondrial dysfunction as an early step of curcumin-induced cell death. These findings corroborate with the reported caspase-9 activation in curcumin-treated T98G cells [16].

Despite the promising results in cell culture models of cancer at concentrations as low as 10 μM, curcumin blood levels are unlikely to reach these concentrations via dietary consumption in humans due to limited mucosal absorption [54]. Oral administration of 8 g/day produced peak blood levels around 2 μM of curcumin in patients [54]. These findings show a gap between the basic and clinical applications of curcumin. On the other hand, studies have found anticancer activities associated with oral, ip and intravenous administration of curcumin in xenografts [55–58]. In our model, we used ip curcumin in order to circumvent the problems associated with its oral absorption. Moreover, ip curcumin may cross the brain blood barrier [57,58]; 50 mg/kg/day was chosen based on the reported literature range (10–120 mg/kg/day) [55–58]. In our model, curcumin significantly reduced the size of brain tumors in C6-implanted rats. Interestingly, curcumin treatment did not induce toxicity to health tissues as evaluated from quantification of serum biomarkers of tissue damage, oxidative stress, hematological parameters and tissue histochemistry. Corroborating with *in vitro* data, these findings suggest a selective toxicity of curcumin against cancer cells *in vivo*. Recently, Perry et al. reported that ip curcumin (60 and 120 mg/kg/day) decreased the subcutaneous growth of U87 tumors in xenografts [58]. In that study, 120 mg/kg/day of curcumin also increased the survival rate in nude mice bearing brain-implanted U87 tumors, although the size of the tumors was not quantified [58]. In brain-implanted B16F10 melanoma cells, tail vein and intracerebral injection of curcumin blocked tumor formation in C57BL6 mice [57]. Therefore, application of injectable formulations of curcumin or direct delivery into the surgical resection cavity could be useful to circumvent the poor oral absorption into a safe therapeutic strategy for treating brain tumors.

This work is the second report of an *in vivo* antiglioma effect of curcumin, but the first using immune-competent rats. The C6 model maintains the immunological and inflammatory surveillances founded *in vivo*, which are critical for gliomas growth and resistance to apoptosis [59]. Perry et al. used immune-compromised mice to implant U87 human cells, and the results also were positive [58]. Given the documented safety of curcumin in humans [54], data presented here and data from Perry et al. provide a provocative foundation for further studies testing and improving the ability of curcumin to limit human brain tumors.

Acknowledgments

We acknowledge the Brazilian funds CAPES, CNPq and FINEP/IBNNet (01060842-00) for financial support.

References

[1] Singh SK, Hawkins C, Clarke ID, Squire JA, Bayani J, Hide T, et al. Identification of human brain tumour initiating cells. Nature 2004;432:396–401.
[2] Legler JM, Ries LA, Smith MA, Warren JL, Heineman EF, Kaplan RS, et al. Cancer surveillance series [corrected]: brain and other central nervous system cancers: recent trends in incidence and mortality. J Natl Cancer Inst 1999; 91:1382–90.
[3] Soni D, King JA, Kaye AH, Hovens CM. Genetics of glioblastoma multiforme: mitogenic signaling and cell cycle pathways converge. J Clin Neurosci 2005;12: 1–5.
[4] Yu C, Friday BB, Yang L, Atadja P, Wigle D, Sarkaria J, et al. Mitochondrial Bax translocation partially mediates synergistic cytotoxicity between histone deacetylase inhibitors and proteasome inhibitors in glioma cells. Neuro Oncol 2008;10(3):309–19.
[5] Brennan C, Momota H, Hambardzumyan D, Ozawa T, Tandon A, Pedraza A, et al. Glioblastoma subclasses can be defined by activity among signal transduction pathways and associated genomic alterations. PLoS One 2009;4(11):e7752.
[6] Roesler R, Brunetto AT, Abujamra AL, de Farias CB, Brunetto AL, Schwartsmann G. Current and emerging molecular targets in glioma. Expert Rev Anticancer Ther 2010;10(11):1735–51.
[7] Gerstner ER, Sorensen AG, Jain RK, Batchelor TT. Anti-vascular endothelial growth factor therapy for malignant glioma. Curr Neurol Neurosci Rep 2009; 9(3):254–62.
[8] Mercer RW, Tyler MA, Ulasov IV, Lesniak MS. Targeted therapies for malignant glioma: progress and potential. BioDrugs 23(1), 25–35.
[9] Singh S, Khar A. Biological effects of curcumin and its role in cancer chemoprevention and therapy. Anticancer Agents Med Chem 2006;6(3):259–70 [Review].
[10] Cheng AL, Hsu CH, Lin JK, Hsu MM, Ho YF, Shen TS, et al. Clinical trial of curcumin, a chemopreventive agent, in patients with high-risk or pre-malignant lesions. Anticancer Res 2001;21:2895–900.
[11] Gao X, Deeb D, Jiang H, Liu YB, Dulchavsky AS, Gautam SC. Curcumin differentially sensitizes malignant glioma cells to TRAIL/Apo2L-mediated apoptosis through activation of procaspases and release of cytochrome c from mitochondria. J Exp Ther Oncol 2005;5:39–48.
[12] Kim SY, Jung SH, Kim HS. Curcumin is a potent broad spectrum inhibitor of matrix metalloproteinase gene expression in human astroglioma cells. Biochem Biophys Res Commun 2005;337:510–6.
[13] Nagai S, Kurimoto M, Washiyama K, Hirashima Y, Kumanishi Y, Endo S. Inhibition of cellular proliferation and induction of apoptosis by curcumin in human malignant astrocytoma cell lines. J Neurooncol 2005;74:105–11.
[14] Woo MS, Jung SH, Kim SY, Hyun JW, Ko KH, Kim WK, et al. Curcumin suppresses phorbol ester-induced matrix metalloproteinase-9 expression by inhibiting the PKC to MAPK signaling pathways in human astroglioma cells. Biochem Biophys Res Commun 2005;335:1017–25.
[15] Belkaid A, Copland IB, Massillon D, Annabi B. Silencing of the human microsomal glucose-6-phosphate translocase induces glioma cell death: potential new anticancer target for curcumin. FEBS Lett 2006;580:3746–52.
[16] Karmakar S, Banik NL, Patel SJ, Ray SK. Curcumin activated both receptor-mediated and mitochondria-mediated proteolytic pathways for apoptosis in human glioblastoma T98G cells. Neurosci Lett 2006;407:53–8.
[17] da Frota Jr ML, Braganhol E, Canedo AD, Klamt F, Apel MA, Mothes B, et al. Brazilian marine sponge *Polymastia janeirensis* induces apoptotic cell death in human U138MG glioma cell line, but not in a normal cell culture. Invest New Drugs 2009;27(1):13–20.
[18] Zanotto-Filho A, Delgado-Cañedo A, Schröder R, Becker M, Klamt F, Moreira JC. The pharmacological NFkappaB inhibitors BAY117082 and MG132 induce cell arrest and apoptosis in leukemia cells through ROS-mitochondria pathway activation. Cancer Lett 2010;288(2):192–203.
[19] Braganhol E, Zamin LL, Cañedo AD, Horn F, Tamajusuku AS, Wink MR, et al. Antiproliferative effect of quercetin in the human U138MG glioma cell line. Anticancer Drugs 2006;17(6):663–71.

[20] Zanotto-Filho A, Gelain DP, Schröder R, Souza LF, Pasquali MA, Klamt F, et al. The NFkappaB-mediated control of RS and JNK signaling in vitamin A-treated cells: duration of JNK-AP-1 pathway activation may determine cell death or proliferation. Biochem Pharmacol 2009;77:1291–301.
[21] Dhandapani KM, Mahesh VB, Brann DWJ. Curcumin suppresses growth and chemoresistance of human glioblastoma cells via AP-1 and NFkappaB transcription factors. J Neurochem 2007;102(2):522–38.
[22] Klamt F, Shacter E. Taurine chloramine, an oxidant derived from neutrophils, induces apoptosis in human B lymphoma cells through mitochondrial damage. J Biol Chem 2005;280:21346–52.
[23] Lin HJ, Su CC, Lu HF, Yang JS, Hsu SC, Ip SW, et al. Curcumin blocks migration and invasion of mouse-rat hybrid retina ganglion cells (N18) through the inhibition of MMP-2, -9, FAK, Rho A and Rock-1 gene expression. Oncol Rep 2010;23(3): 665–70.
[24] Uliasz TF, Hewett SJ. A microtiter trypan blue absorbance assay for the quantitative determination of excitotoxic neuronal injury in cell culture. J Neurosci Methods 2000;100(1–2):157–63.
[25] Takano T, Lin JHC, Arcuino G, Gao Q, Yang J, Nedergaard M. Glutamate release promotes growth of malignant gliomas. Nature Med 2001;7:1010–5.
[26] Morrone FB, Oliveira DL, Gamermann P, Stella J, Wofchuk S, Wink MR, et al. In vivo glioblastoma growth is reduced by apyrase activity in a rat glioma model. BMC Cancer 2006;6:226–36.
[27] Braganhol E, Morrone FB, Bernardi A, Huppes D, Meurer L, Edelweiss MI, et al. Selective NTPDase2 expression modulates in vivo rat glioma growth. Cancer Sci 2009;100(8):1434–42.
[28] De Oliveira MR, Moreira JC. Impaired redox state and respiratory chain enzyme activities in the cerebellum of vitamin A-treated rats. Toxicology 2008;253(1–3): 125–30.
[29] Brown RE, Law A. Morphoproteomic demonstration of constitutive nuclear factor-kappaB activation in glioblastoma multiforme with genomic correlates and therapeutic implications. Ann Clin Lab Sci 2006;36(4):421–6.
[30] Gao X, Deeb D, Jiang H, Liu Y, Dulchavsky SA, Gautam SC. Synthetic triterpenoids inhibit growth and induce apoptosis in human glioblastoma and neuroblastoma cells through inhibition of prosurvival Akt, NF-kappaB and Notch1 signaling. J Neurooncol 2007;84(2):147–57.
[31] Nakanishi C, Toi M. Nuclear factor-kappaB inhibitors as sensitizers to anticancer drugs. Nat Rev Cancer 2005;5(4):297–309.
[32] Yahanda AM, Bruner JM, Donehower LA, Morrison RS. Astrocytes derived from p53-deficient mice provide a multistep in vitro model for development of malignant gliomas. Mol. Cell Biol 1995;15:4249–59.
[33] Lowe SW, Bodis S, McClatchey A, Remington L, Ruley HE, Fisher DE, et al. p53 Status and the efficacy of cancer therapy in vivo. Science 1994;266:807–10.
[34] Lowe SW, Ruley HE, Jacks T, Housman DE. p53-Dependent apoptosis modulates the cytotoxicity of anticancer agents. Cell 1993;74:957–67.
[35] Devarajan E, Sahin AA, Chen JS, Krishnamurthy RR, Aggarwal N, Brun AM, et al. Down-regulation of caspase 3 in breast cancer: a possible mechanism for chemoresistance. Oncogene 2002;21:8843–51.
[36] Igney FH, Krammer PH. Death and anti-death: tumour resistance to apoptosis. Nat. Rev Cancer 2002;2:277–88.
[37] Jaattela M. Multiple cell death pathways as regulators of tumour initiation and progression. Oncogene 2004;23:2746–56.
[38] Ansari SA, Safak M, Del Valle L, Enam S, Amini S, Khalili K. Cell cycle regulation of NF-kappa b-binding activity in cells from human glioblastomas. Exp. Cell Res 2001;265:221–33.
[39] Bredel M, Bredel C, Juric D, Duran GE, Yu RX, Harsh GR, et al. Tumor necrosis factor-alpha-induced protein 3 as a putative regulator of nuclear factor-kappaB-mediated resistance to O6-alkylating agents in human glioblastomas. J Clin Oncol 2006;24(2):274–87.
[40] Wang H, Wang H, Zhang W, Huang HJ, Liao WS, Fuller GN. Analysis of the activation status of Akt, NFkappaB, and Stat3 in human diffuse gliomas. Lab Invest 2004;84(8):941–51.
[41] Park S, Hatanpaa KJ, Xie Y, Mickey BE, Madden CJ, Raisanen JM, et al. The receptor interacting protein 1 inhibits p53 induction through NF-kappaB activation and confers a worse prognosis in glioblastoma. Cancer Res 2009;69(7):2809–16.
[42] Sethi G, Ahn KS, Chaturvedi MM, Aggarwal BB. Epidermal growth factor (EGF) activates nuclear factor-kappaB through IkappaBalpha kinase-independent but EGF receptor-kinase dependent tyrosine 42 phosphorylation of IkappaBalpha. Oncogene 2007;26(52):7324–32.
[43] Raychaudhuri B, Han Y, Lu T, Vogelbaum MA. Aberrant constitutive activation of nuclear factor kappaB in glioblastoma multiforme drives invasive phenotype. J Neurooncol 2007;85(1):39–47.
[44] Robe PA, Bentires-Alj M, Bonif M, Rogister B, Deprez M, Haddada H, et al. In vitro and in vivo activity of the nuclear factor-kappaB inhibitor sulfasalazine in human glioblastomas. Clin Cancer Res 2004;10(16):5595–603.
[45] Sansal I, Sellers WR. The biology and clinical relevance of the PTEN tumor suppressor pathway. J Clin Oncol 2004;22(14):2954–63.
[46] Lim GP, Chu T, Yang F, Beech W, Frautschy SA, Cole GM. The curry spice curcumin reduces oxidative damage and amyloid pathology in an Alzheimer transgenic mouse. J Neurosci 2001;21:8370–7.
[47] Thiyagarajan M, Sharma SS. Neuroprotective effect of curcumin in middle cerebral artery occlusion induced focal cerebral ischemia in rats. Life Sci 2004;74:969–85.
[48] Opel D, Westhoff MA, Bender A, Braun V, Debatin KM, Fulda S. Phosphatidylinositol 3-kinase inhibition broadly sensitizes glioblastoma cells to death receptor- and drug-induced apoptosis. Cancer Res 2008;68(15):6271–80.
[49] Weaver KD, Yeyeodu S, Cusack Jr JC, Baldwin AS, Ewend MG. Potentiation of chemotherapeutic agents following antagonism of nuclear factor kappa B in human gliomas. J Neurooncol 2003;61:187–96.
[50] Stewart LA. Chemotherapy in adult high-grade glioma: a systematic review and meta-analysis of individual patient data from 12 randomised trials. Lancet 2002;359:1011–8.
[51] Nagane M, Levitzki A, Gazit A, Cavenee WK, Huang HJ. Drug resistance of human glioblastoma cells conferred by a tumor-specific mutant epidermal growth factor receptor through modulation of Bcl-XL and caspase-3-like proteases. Proc Natl Acad Sci USA 1998;95:5724–9.
[52] Cheng Q, Lee HH, Li Y, Parks TP, Cheng G. Upregulation of Bcl-x and Bfl-1 as a potential mechanism of chemoresistance, which can be overcome by NF-kappaB inhibition. Oncogene 2000;19:4936–40.
[53] Jiang Z, Zheng X, Rich KM. Down-regulation of Bcl-2 and Bcl-xL expression with bispecific antisense treatment in glioblastoma cell lines induce cell death. J Neurochem 2003;84:273–81.
[54] Anand P, Kunnumakkara AB, Newman RA, Aggarwal BB. Bioavailability of curcumin: problems and promises. Mol Pharm 2007;4(6):807–18 [Review].
[55] Shankar S, Ganapathy S, Chen Q, Srivastava RK. Curcumin sensitizes TRAIL resistant xenografts: molecular mechanisms of apoptosis, metastasis and angiogenesis. Mol Cancer 2008;7:16–29.
[56] Dujic J, Kippenberger S, Ramirez-Bosca A, Diaz-Alperi J, Bereiter-Hahn J, Kaufmann R, et al. Curcumin in combination with visible light inhibits tumor growth in a xenograft tumor model. Int J Cancer 2009;124(6):1422–8.
[57] Purkayastha S, Berliner A, Fernando SS, Ranasinghe B, Ray I, Tariq H, et al. Curcumin blocks brain tumor formation. Brain Res 2009;1266:130–8.
[58] Perry MC, Demeule M, Régina A, Moumdjian R, Béliveau R. Curcumin inhibits tumor growth and angiogenesis in glioblastoma xenografts. Mol Nutr Food Res 2010;54:1–10.
[59] Albesiano E, Han JE, Lim M. Mechanisms of local immunoresistance in glioma. Neurosurg Clin N Am 2010;21(1):17–29.